Nitro group and K^+ based secondary building unit for the self-assembly of 3D coordination polymers built on dinuclear dianionic helicate connectors.

Raúl Mendoza-Báez, Alan Molina-Renteria, and Juan Olguín*

Departamento de Química, Centro de Investigación y de Estudios Avanzados del IPN (Cinvestav), Avenida IPN 2508, Col. San Pedro Zacatenco, Ciudad de México 07360, México.

e-mail jolguin@cinvestav.mx

Supplementary Information

Contents

1. X-ray analysis

1.1 Structural refinement details for complexes

X-ray diffraction measurements were collected on a Bruker D8 VENTURE diffractometer (PHOTON 100 detector), using multilayer mirror monochromator and MoKα source (λ = 0.71073 Å). Data collection, cell refinement, and data reduction were done with Bruker APEX 3 suite. The structural refinement was carried out by a full-matrix least-squares method based on F2 and using SHELXL 2019/3 with SHELXLE (rev. 1569) graphical user interface.[S1] Absorption corrections were performed by Multi-Scan. All non-hydrogen atoms were refined with anisotropic thermal displacement coefficients.

The structure of complex **1** at room temperature shows a methanol solvent molecule disordered over two positions, found in a 0.60/0.40 occupancy for C(42)-O(10)/C(43)-O(11), respectively. The SIMU and ISOR commands were applied for both parts of the disorder modeling. The crystal structure of **2** at room temperature shows a one-half acetonitrile molecule and no structural constraints were employed.

The check cif for complex 2 shows an alert A:

```
PLAT601_ALERT_2_A Structure Contains Solvent Accessible VOIDS of . 219 Ang**3
```

Which is due to the rigid reticular 3D structure.

Table S1. Crystal data and structure refinement for complex **1**

Identification code	AMR24TAKMeOH	
Empirical formula	C_{83} H_{62} K_2 Mn_2 N_{12} O_{20}	
Formula weight	1735.52	
Temperature	298(2) K	
Wavelength	0.71073 Å	
Crystal system	Monoclinic	
Space group	C2/c	
Unit cell dimensions	a = 16.080(3) Å	a= 90°.
	b = 14.472(3) Å	b= 100.611(8)°
	c = 37.326(8) Å	g = 90°.
Volume	8537(3) Å3	
Z	4	
Density (calculated)	1.350 Mg/m3	
Absorption coefficient	0.469 mm-1	
F(000)	3568	
Crystal size	0.350 x 0.260 x 0.100 mm3	
Theta range for data collection	2.221 to 27.195°.	
Index ranges	-20 ≤ h ≤ 20, -18 ≤ k ≤ 18, -47 ≤ l ≤ 47	
Reflections collected	126744	
Independent reflections	9469 [R(int) = 0.1708]	
Completeness to theta = 25.242°	99.7 %	
Absorption correction	Semi-empirical from equivalents	
Max. and min. transmission	0.7455 and 0.4820	
Refinement method	Full-matrix least-squares on F2	
Data / restraints / parameters	9469 / 36 / 558	
Goodness-of-fit on F2	1.026	
Final R indices [I>2sigma(I)]	R1 = 0.0737, wR2 = 0.1871	
R indices (all data)	R1 = 0.1797, wR2 = 0.2480	
Largest diff. peak and hole	0.851 and -0.356 e.Å-3	

Table S2. Crystal data and structure refinement for complex **2**

Identification code	JOAMR137B	
Empirical formula	C_{83} H_{57} K_2 N_{13} Ni_2 O_{18}	
Formula weight	1720.03	
Temperature	296(2) K	
Wavelength	0.71073 Å	
Crystal system	Monoclinic	
Space group	C2/c	
Unit cell dimensions	a = 15.7610(11) Å	α = 90 °
	b = 14.5644(9) Å	β = 97.921(2) °
	c = 36.558(3) Å	γ = 90 °
Volume	8311.7(10) Å3	
Z	4	
Density (calculated)	1.375 Mg/m^3	
Absorption coefficient	0.629 mm^{-1}	
F(000)	3536	
Crystal size	0.384 x 0.217 x 0.056 mm^3	
Theta range for data collection	2.250 to 25.026 °	
Index ranges	$-18 \leq h \leq 18$	
	$-17 \leq k \leq 17$	
	$-42 \leq l \leq 43$	
Reflections collected	204178	
Independent reflections	7322 [R(int) = 0.1132]	
Completeness to theta = 25.026°	99.6 %	
Absorption correction	Semi-empirical from equivalents	
Max. and min. transmission	0.7452 and 0.6704	
Refinement method	Full-matrix least-squares on F^2	
Data / restraints / parameters	7322 / 0 / 551	
Goodness-of-fit on F^2	1.066	
Final R indices [I>2sigma(I)]	R_1 = 0.0642, wR_2 = 0.1671	
R indices (all data)	R_1 = 0.1076, wR_2 = 0.1879	
Largest diff. peak and hole	0.795 and -0.267 e.$Å^{-3}$	

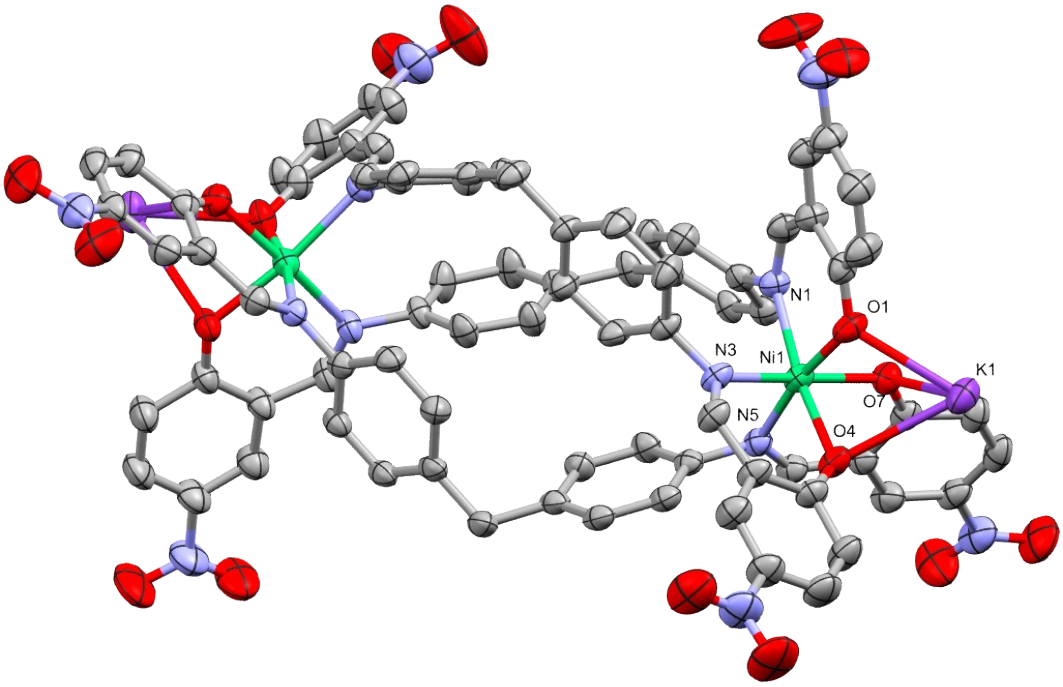

Figure S1. Perspective view of $K_2[Ni^{II}L_3]\cdot MeCN$ (**2**) acquired at 296 K, with ellipsoids drawn at 40% probability level. Solvent molecule and hydrogen atoms are omitted for the sake of clarity.

Table S3. M^{II}—N/O_{donors} bond length and angles of the $M^{II}\{N_3O_3\}$ coordination sphere in **1** (left) and **2** (right).

Bond	Distance (Å) / Angle (°)	Bond	Distance (Å) / Angle (°)
Mn(1)-O(4)#3	2.106(3)	Ni(1)-O(4)#2	2.042(3)
Mn(1)-O(7)	2.119(3)	Ni(1)-O(7)	2.043(3)
Mn(1)-O(1)	2.123(3)	Ni(1)-O(1)	2.037(3)
Mn(1)-N(5)	2.274(4)	Ni(1)-Ni(5)	2.116(4)
N(1)-N(1)	2.285(4)	Ni(1)-N(1)	2.132(3)
Mn(1)-N(3)#3	2.321(4)	Ni(1)-N(3)#2	2.126(3)
O(4)#3-Mn(1)-O(7)	85.21(14)	O(1)-Ni(1)-O(4)#2	84.97(12)
O(4)#3-Mn(1)-O(1)	86.95(14)	O(1)-Ni(1)-O(7)	85.87(12)
O(7)-Mn(1)-O(1)	89.04(13)	O(4)#2-Ni(1)-O(7)	85.84(12)
O(4)#3-Mn(1)-N(5)	167.95(14)	O(1)-Ni(1)-N(5)	170.94(12)
O(7)-Mn(1)-N(5)	82.88(13)	O(4)#2-Ni(1)-N(5)	87.24(13)
O(1)-Mn(1)-N(5)	91.03(13)	O(7)-Ni(1)-N(5)	88.95(13)
O(4)#3-Mn(1)-N(1)	89.87(14)	O(1)-Ni(1)-N(3)#2	86.02(13)
O(7)-Mn(1)-N(1)	170.62(13)	O(4)#2-Ni(1)-N(3)#2	89.37(12)
O(1)-Mn(1)-N(1)	82.72(13)	O(7)-Ni(1)-N(3)#2	170.91(12)
N(5)-Mn(1)-N(1)	101.67(13)	N(5)-Ni(1)-N(3)#2	98.55(13)
O(4)#3-Mn(1)-N(3)#3	80.85(13)	O(1)-Ni(1)-N(1)	87.83(12)
O(7)-Mn(1)-N(3)#3	92.66(13)	O(4)#2-Ni(1)-N(1)	171.72(13)
O(1)-Mn(1)-N(3)#3	167.49(13)	O(7)-Ni(1)-N(1)	89.58(13)
N(5)-Mn(1)-N(3)#3	101.47(13)	N(5)-Ni(1)-N(1)	99.58(13)
N(1)-Mn(1)-N(3)#3	94.44(13)	N(3)#2-Ni(1)-N(1)	94.21(13)

Symmetry transformations used to generate equivalent atoms:

In complex **1**: #3 -x+1,y,-z+1/2 ; In complex **2**: #2 -x+1,y,-z+1/2

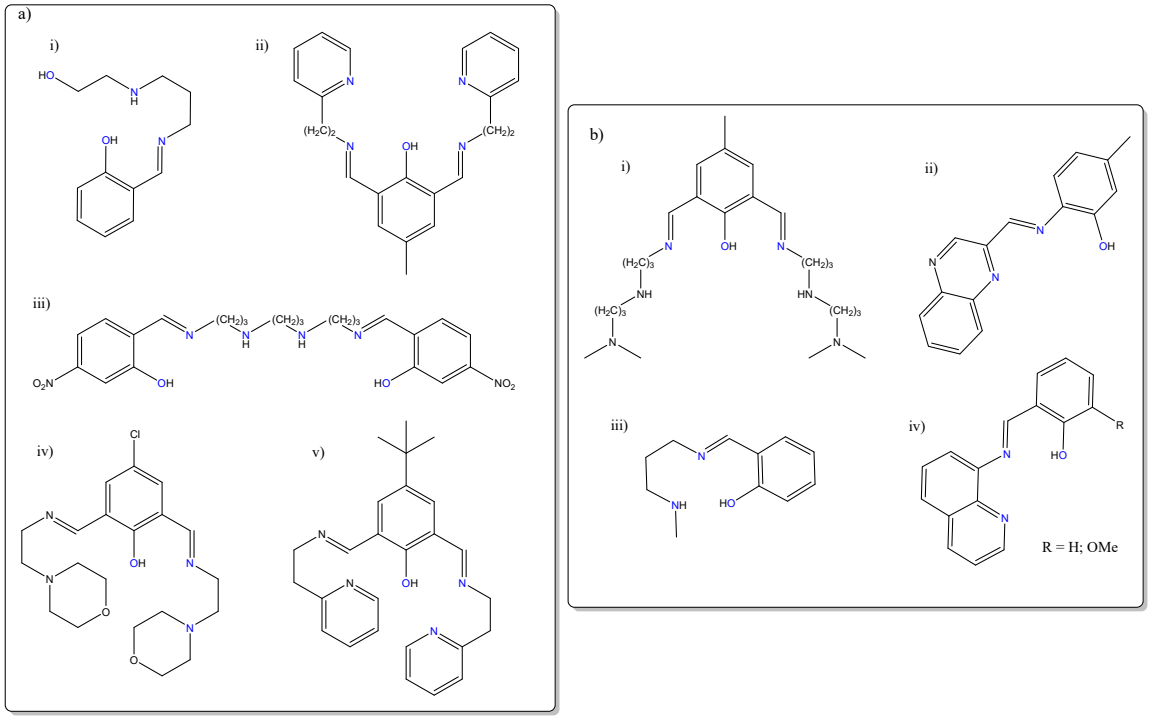

Figure S2. Salicylimine-based ligands used in six-coordinate complexes of (a) Mn^{II} (high-spin, S = 5/2) and (b) Ni^{II}. In blue the donor atoms that participate in the coordination to the metal.[S2, S3, S4, S5, S6, S7, S8, S9, S10]

2. Solvent molecule-potassium interactions

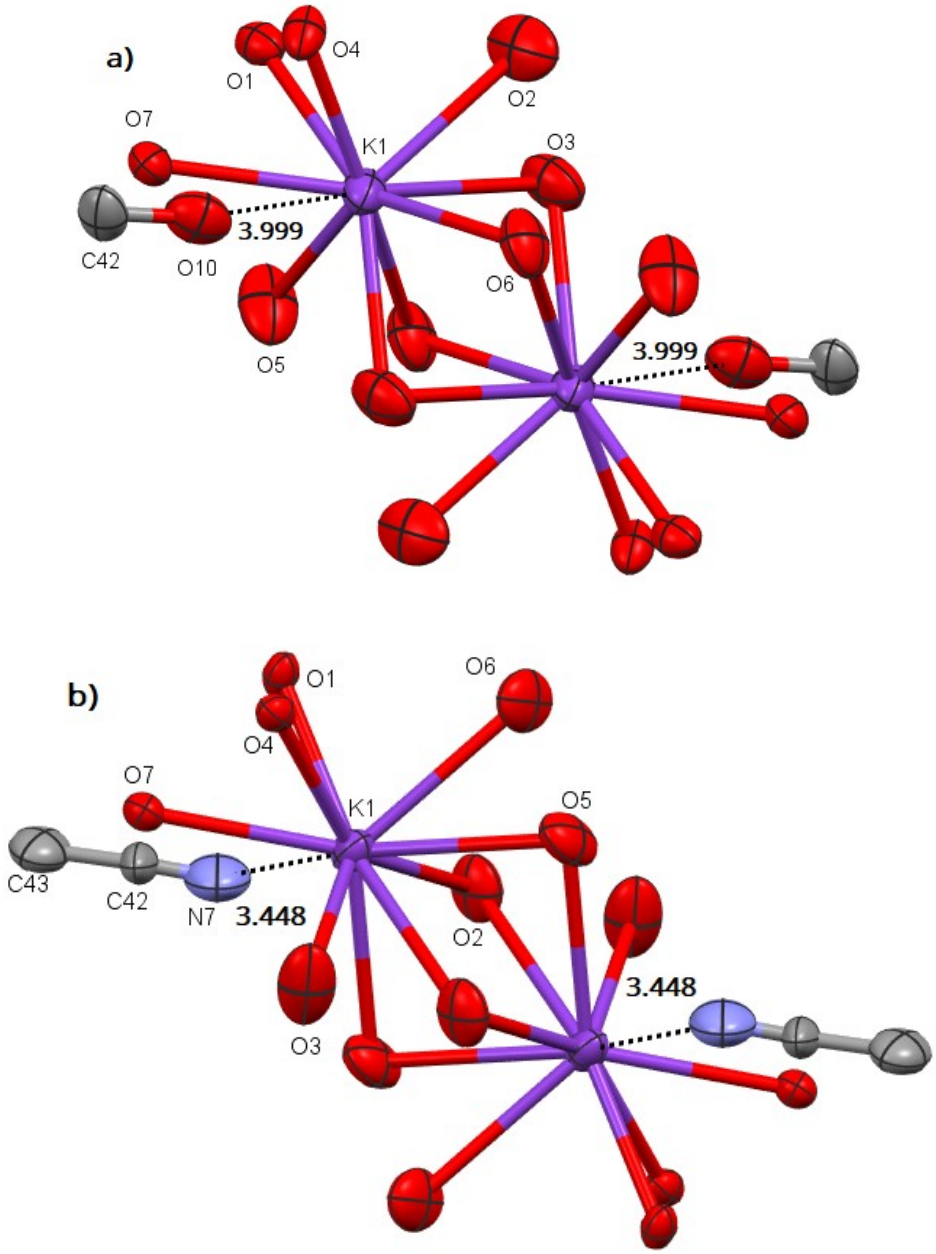

Figure S3. Perspective view of nine-coordinate potassium atoms in (a) complex **1** and (b) complex **2**, with ellipsoids drawn at 30% probability level. Hydrogen atoms are omitted for the sake of clarity. Black dashed line as K— $X_{solvent}$ distance in Å (X = O_{MeOH}, N_{MeCN}).

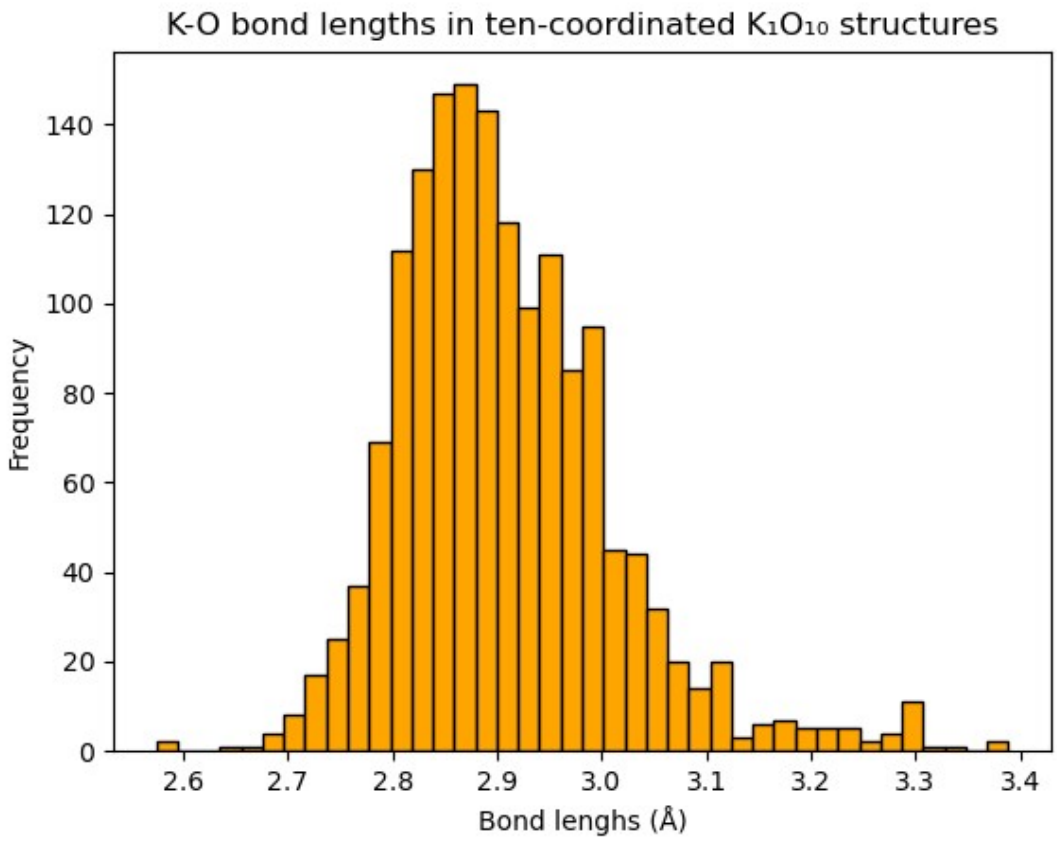

Figure S4. Histogram of K—O bond lengths (in Å) in ten-coordinated KO_{10} structures found in CSD database (update June 2023).

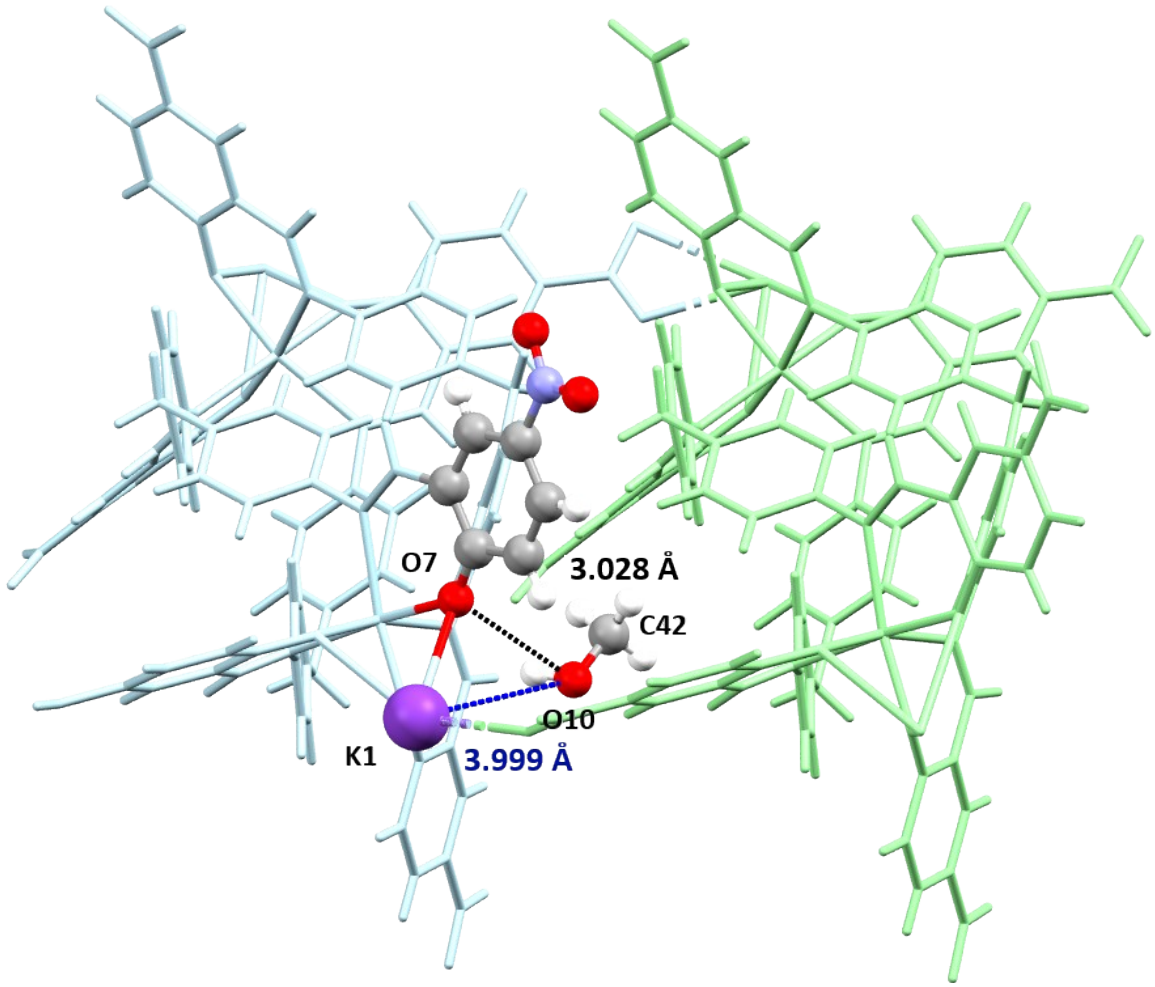

Figure S5. Non-covalent interactions of the methanol molecule in complex **1**: K—O_{MeOH} (blue dashed line, 3.999(7) Å) and O_{10}-H···$O_{phenolate}$ hydrogen bond (black dashed line, 3.028(7) Å). The MeOH molecule is located between two helicate units (green and blue capped stick-style structures) connected by the potassium atom.

3. 3D packing and metal-metal distances

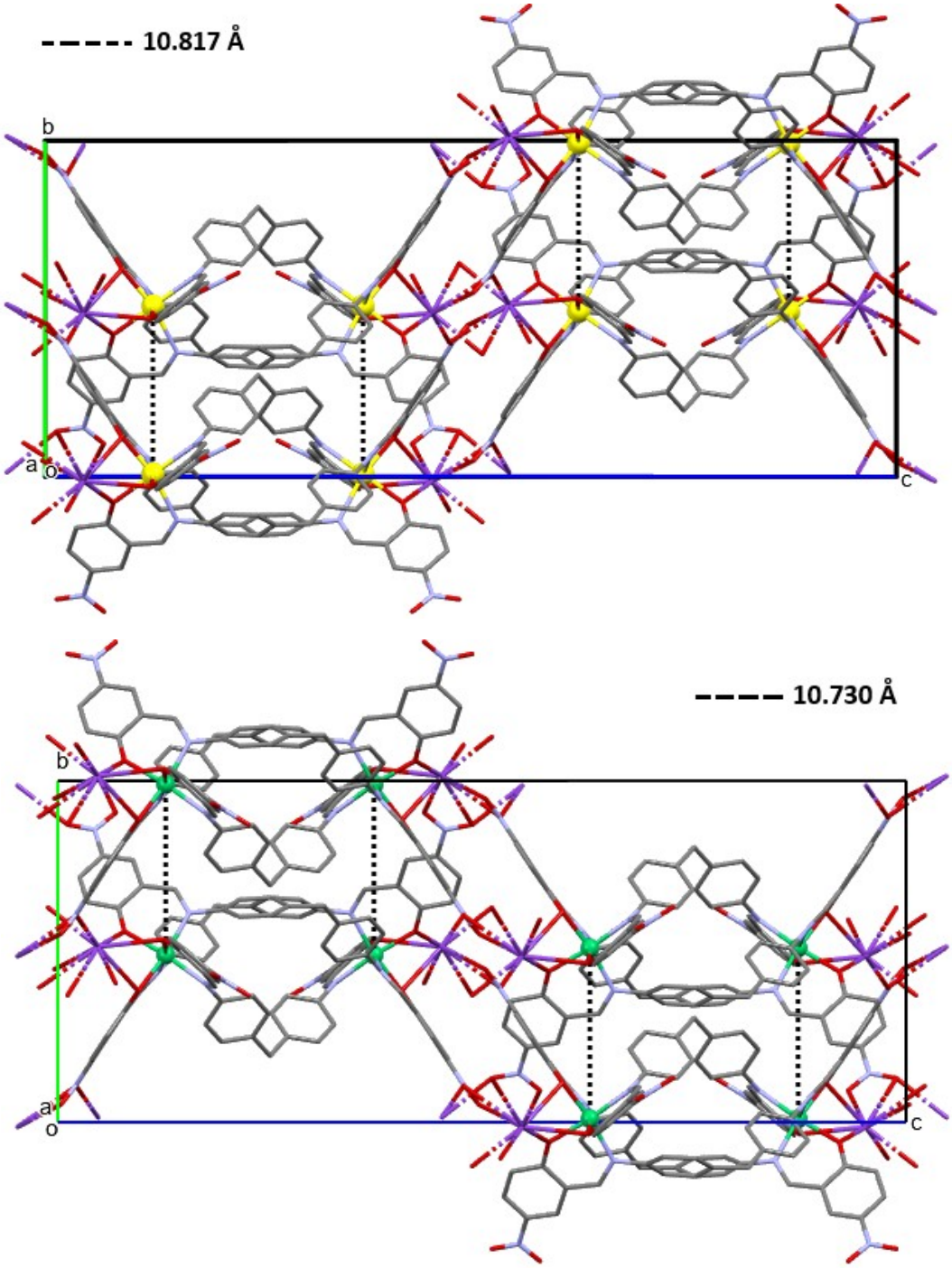

Figure S6. Intermolecular TM—TM interaction (black dashed line) parallel to the *ab* plane, seen along the *a* axis. Top: Complex **1**, with distance of 10.817 Å. Bottom: Complex **2**, with distance of 10.730 Å. The Mn and Ni atoms are in yellow and green balls, respectively, while the rest of the atoms are in a capped stick style. The hydrogen atoms and solvent molecule have been omitted for the sake of clarity.

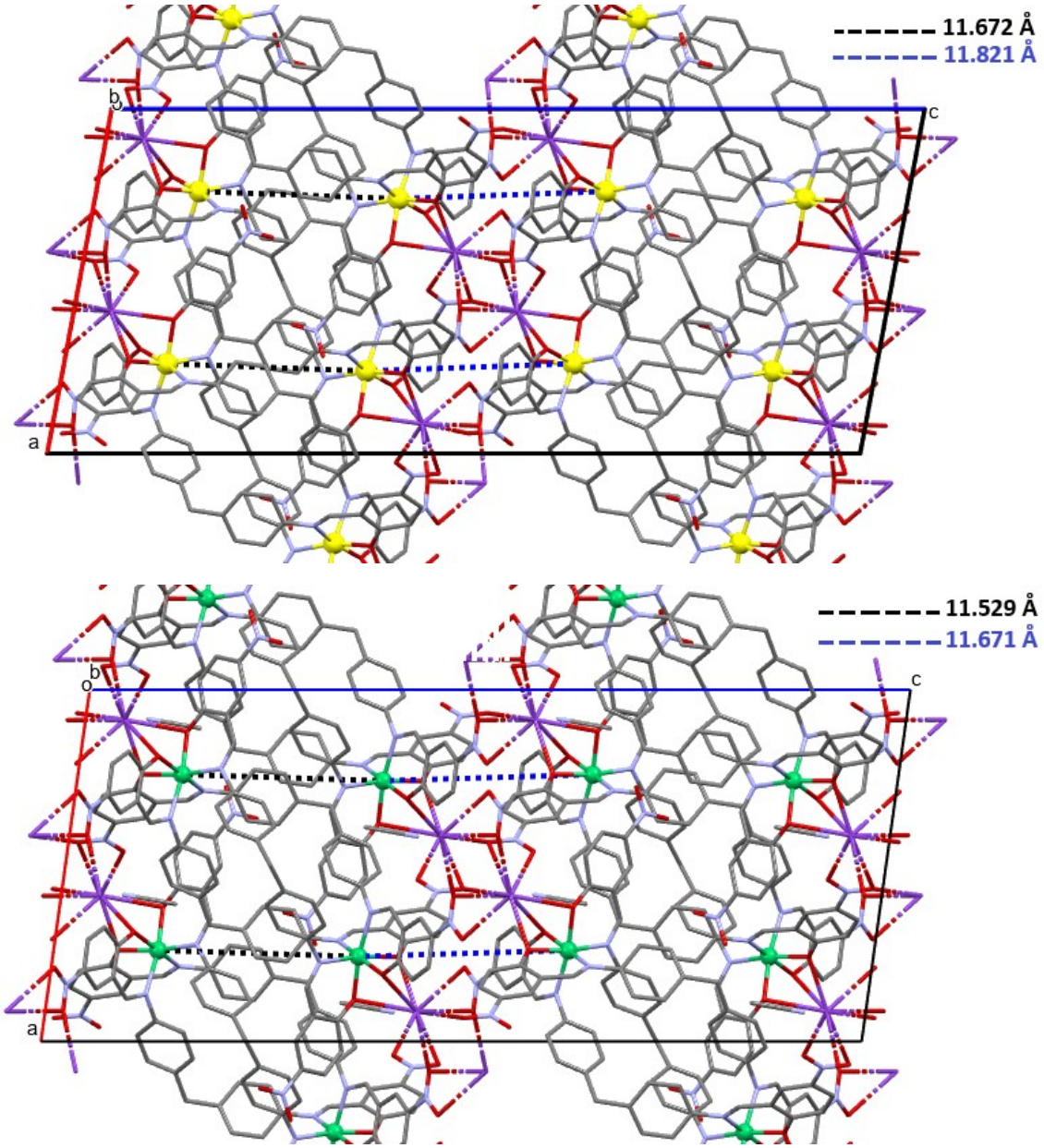

Figure S7. Intermolecular TM—TM interactions parallel to the *bc* plane, seen along the *b* axis. Top: Complex **1**, with distances of 11.672 Å and 11.821 Å (black and blue dashed lines, respectively). Bottom: Complex **2**, with distances of 11.529 Å and 11.671 Å (black and blue dashed lines, respectively). The Mn and Ni atoms are in yellow and green balls, respectively, while the rest of the atoms are in a capped stick style. The hydrogen atoms and solvent molecule have been omitted for the sake of clarity.

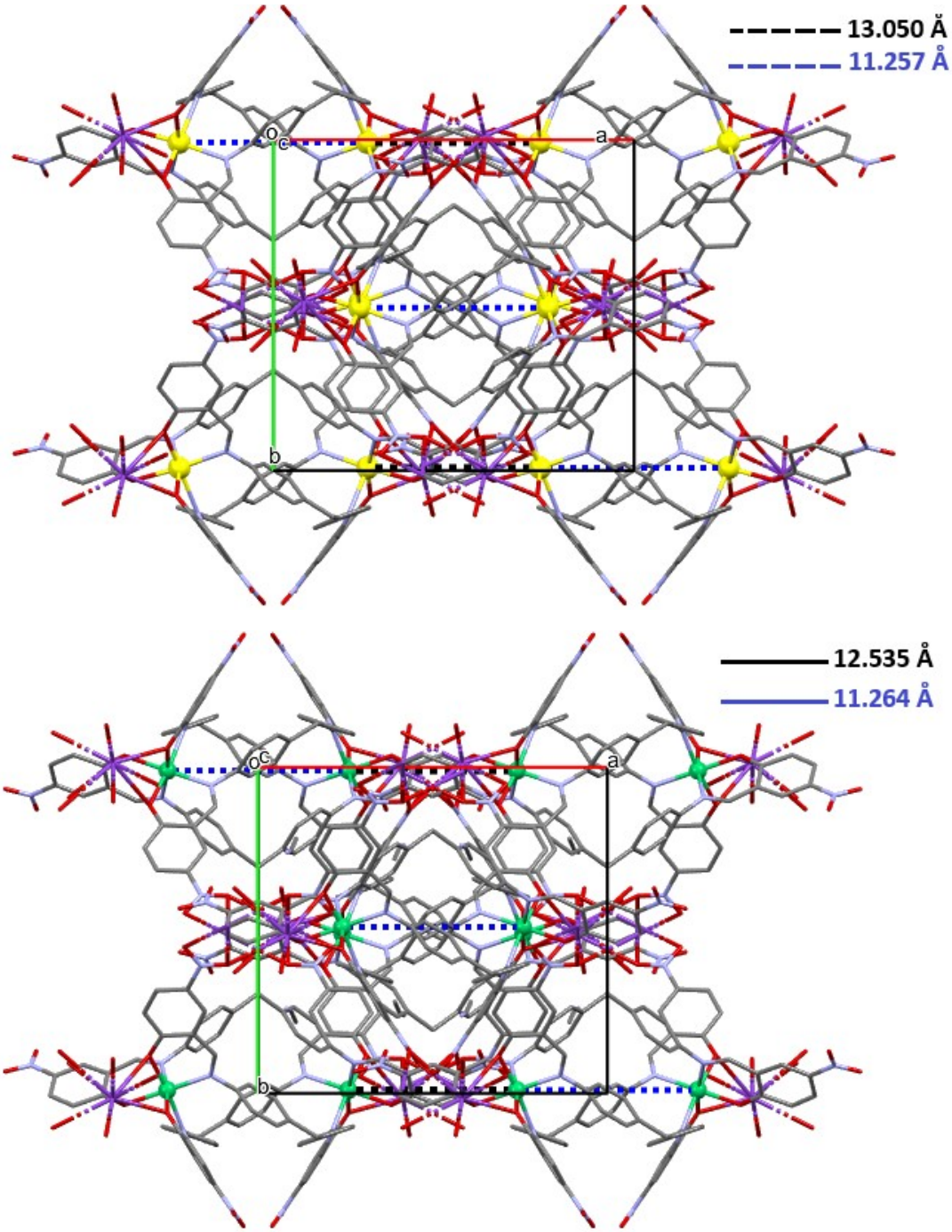

Figure S8. Inter- and intramolecular TM—TM interactions parallel to the *ac* plane, seen along the *c* axis. Top: complex **1**, with distances of 11.257 Å and 13.050(2) Å (blue and black dashed lines, respectively). Bottom: complex **2**, with distances of 11.264 Å and 12.535 Å (blue and black dashed lines, respectively). The Mn and Ni atoms are in yellow and green balls, respectively, while the rest of the atoms are in a capped stick style. The hydrogen atoms and solvent molecule have been omitted for the sake of clarity.

Table S4. M—M distances (in Å) of the closest contacts between the transition metals (Mn^{II} or Ni^{II}) in complexes **1** and **2**.

Complex	**1**	**2**
‖ to *ab* plane	10.817(2)	10.730(1)
‖ to *bc* plane	11.672(2)	11.529(1)
‖ to *bc* plane	11.821(2)	11.671(1)
‖ to *ac* plane	11.257(2)	11.264(1)
‖ to *ac* plane	13.050(2)	12.535(1)

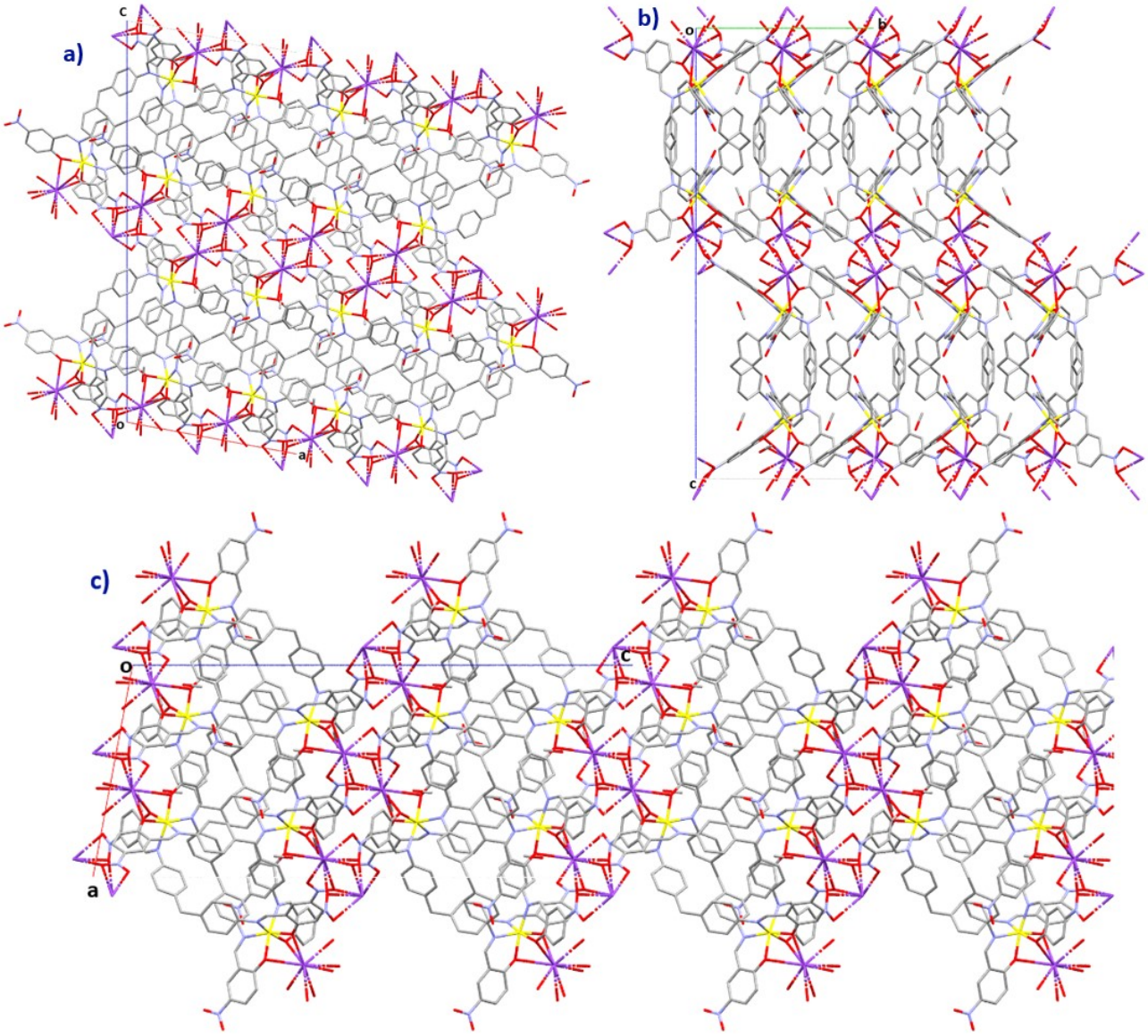

Figure S9. Crystalline packing of $K_2[Mn^{II}L_3]\cdot MeOH$ (**1**), in a capped stick style. (a) Growth along the *a* axis, seen through the *b* axis; (b) growth along the *b* axis, seen through the *a* axis; (c) growth along the *c* axis, seen through the *b* axis. The hydrogen atoms have been omitted for the sake of clarity.

4. Non-covalent interactions

There is another non-covalent interaction that promotes the 3D growth of the crystal structure, that is, the intermolecular π—π stacking between two aromatic rings of terminal nitrophenolate groups, as shown in Fig. S10. This interaction is an off-centered parallel stacking with an interplanar angle of 0.0°. There is an interplanar normal distance about 3.51—3.53 Å and a horizontal displacement (offset) of 2.30—2.39 Å (Figs. S11-S12). Both normal and offset distances agree with the range of typical distances reported in other π—π stacking systems.S[11,] S[12] These π—π interactions, together with the coordinated K atoms, promote the structural growth of zigzag-type chains along the *c* axis, Fig. S13. Furthermore, intramolecular C-H/π interactions occur in complexes **1** and **2**, where a C(sp^2)-H of a benzene ring from diphenylmethane moiety is directed towards the benzene center of and adjacent ligand strand (Figs. S14-S15). Both aromatic rings of a single diphenylmethane moiety act as the C-H/π acceptor, while the remaining two ligands act as the donors. The C-H/π distances are 3.640 and 3.503 Å for complexes **1** and **2**, respectively. The interplanar angles close to 90° (87.27° and 88.89°), as well as the C-H- π α angle close to 180° (167.46° and 168.80°) indicate a *quasi*-perpendicular interaction (Fig. S16).

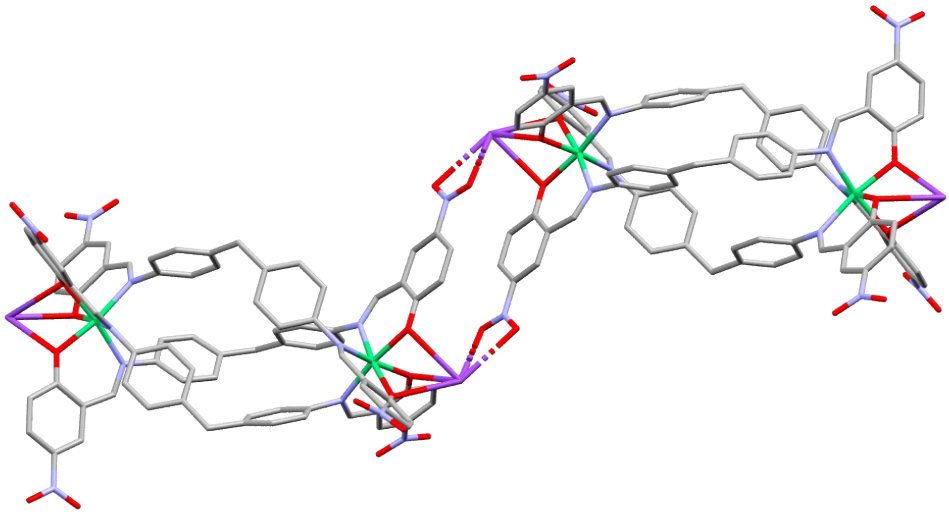

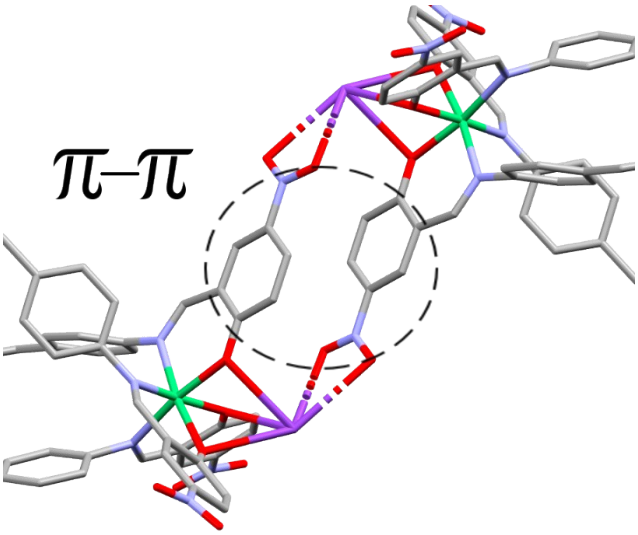

Figure S10. (a) Perspective view of two $K_2[Ni^{II}L_3]\cdot MeCN$ (**2**) molecules, as example, showing the intermolecular π—π stacking between two aromatic rings from nitro-phenolate. (b) Close-up on π—π stacking. The capped sticks style and omission of hydrogen atoms was done for the sake of clarity. Atom color notation: O – red, N – blue, K – purple, Ni – green, C – gray.

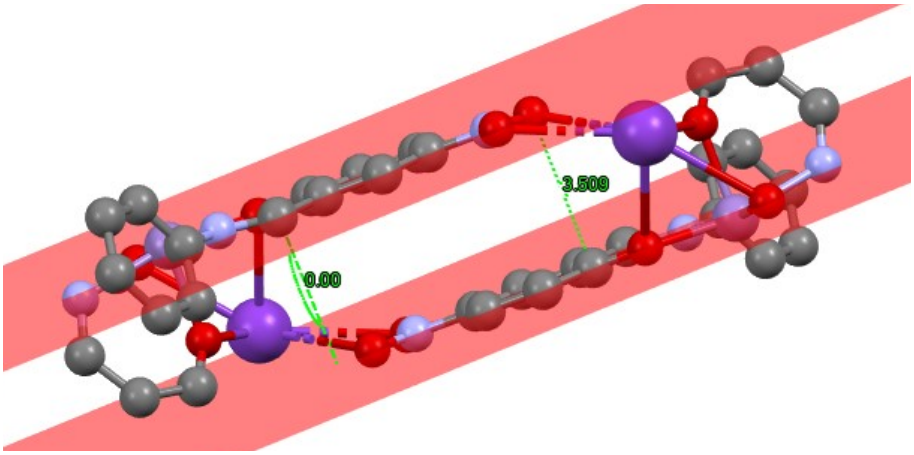

Figure S11. Planes formed by the π-π interacting phenyl units for complex **1**.

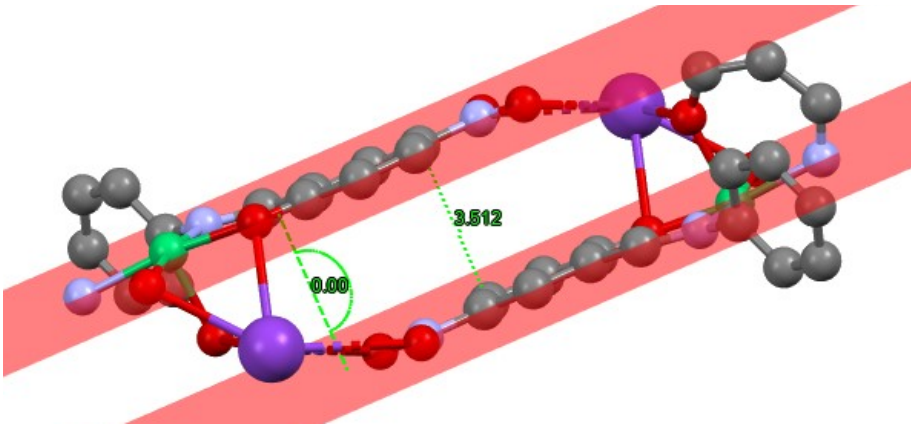

Figure S12. Planes formed by the π-π interacting phenyl units for complex **2**.

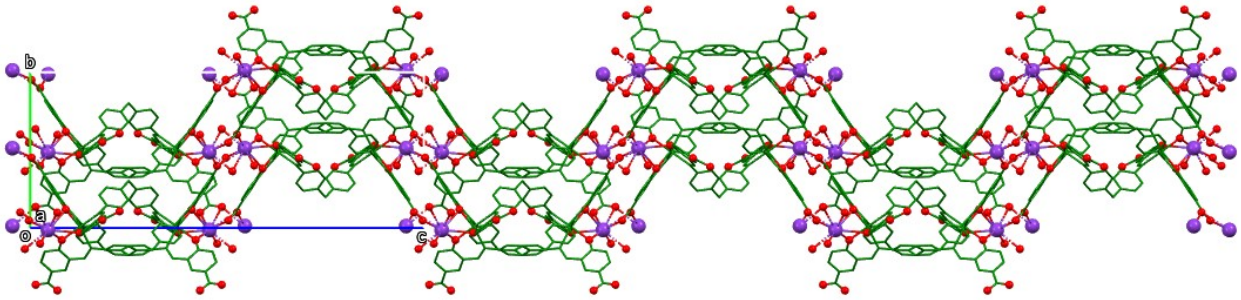

Figure S13. Structure seen along the *a* axis of the zigzag chain growing along the *c* axis (complex **1** as an example). Potassium-oxygen dinuclear units in balls and sticks style, while the rest of the atoms in green capped sticks. The solvent molecule and hydrogen atoms have been omitted.

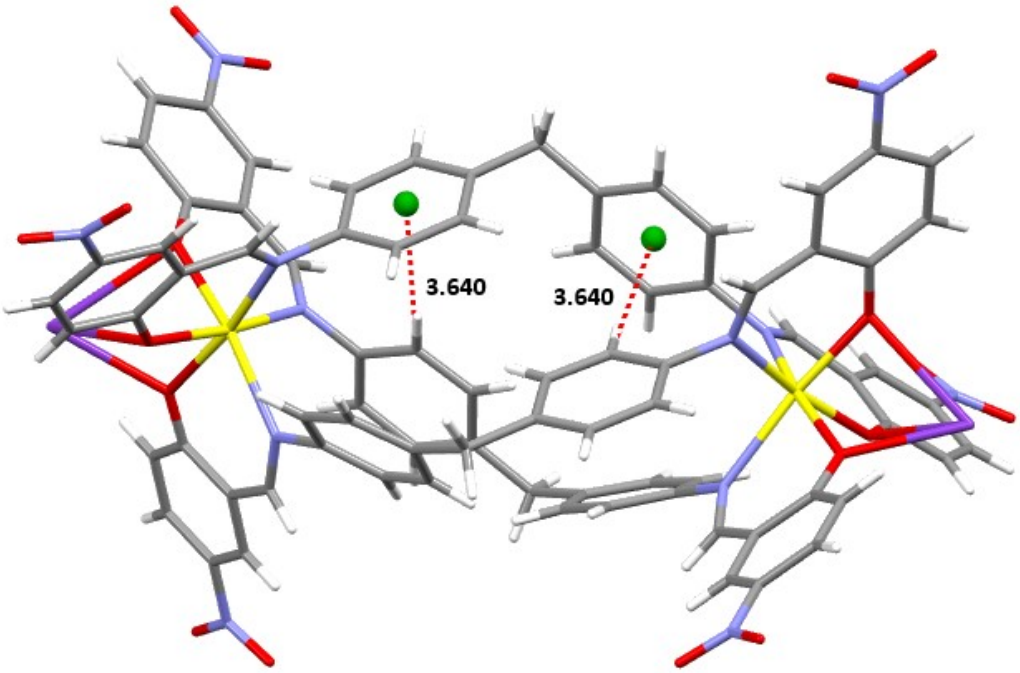

Figure S14. C-H/π interaction in complex **1**. Green sphere as aromatic ring centroid and red dashed line as C_{donor}—centroid distance in Å.

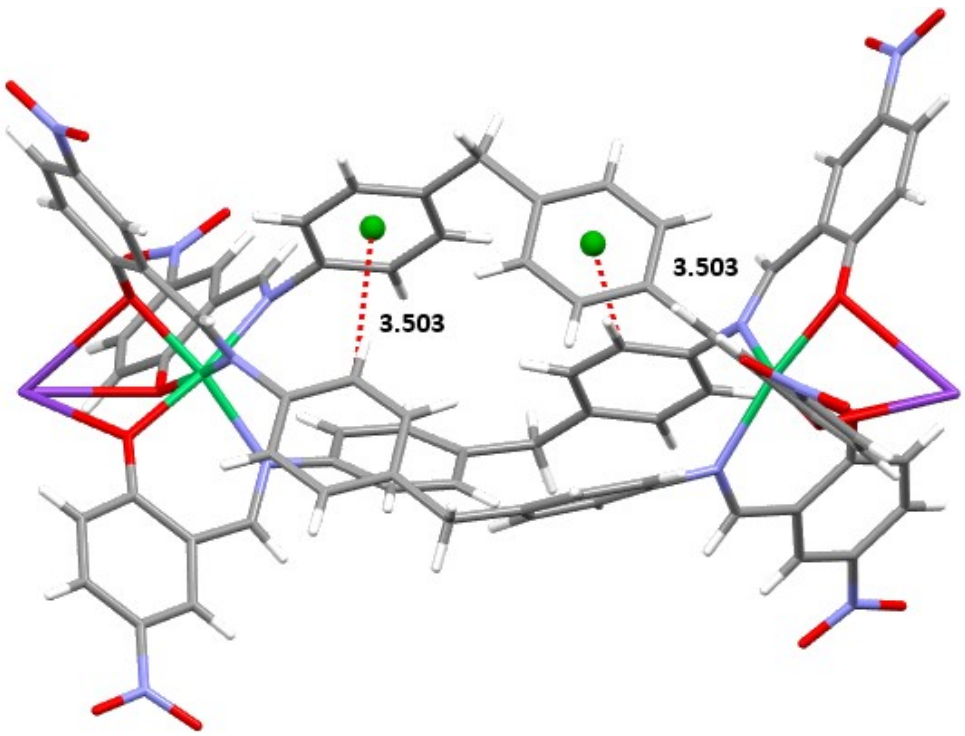

Figure S15. C-H/π interaction in complex **2**. Green sphere as aromatic ring centroid and red dashed line as C_{donor}—centroid distance in Å.

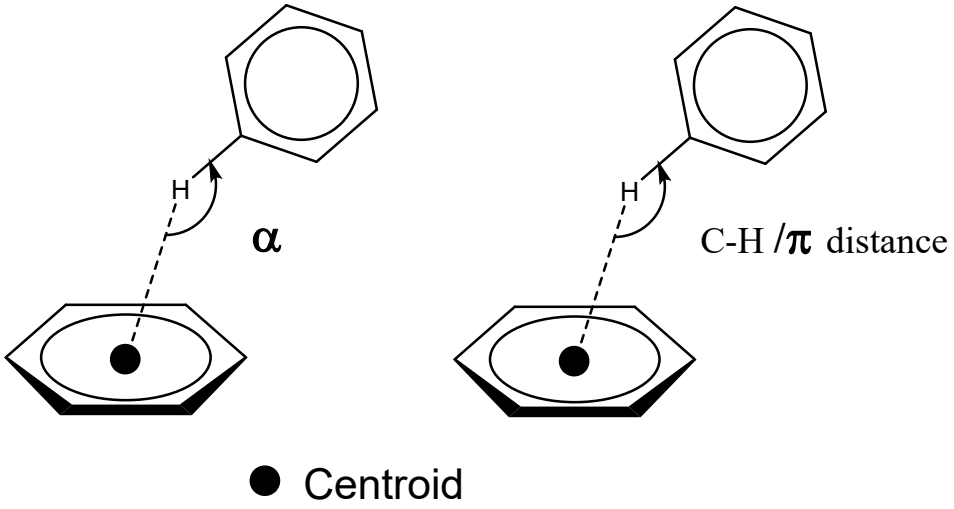

Figure S16. Schematic representation of the structural parameters that describe the C-H/ π interaction: (left) C-H- π α angle and (right) distance from the C-H carbon to the ring centroid.

5. CSD Database Information

Table S5. Crystal structures that contain a nitro aromatic group coordinated to a metal atom. The structures containing metalloligands coordinated to the metal cation are highlighted in blue.

Metal	Coordination Mode	NO_2 groups per $[M^+]$ [a]	Dimensional Arrangement	Is the multidimensional arrangement due to the NO_2 group?	CCDC number
Na	M, B	2	2D	Yes	961952
Na	M, B	2	3D	Yes	1001668
Na	B	1	3D	Yes	602007
Na	B	1	3D	Yes	885242
Na	B	1	2D	Yes	1430370
Na	B	1	2D	Yes	764992
Na	M, B	2	2D	Yes	2064919
Na	B	1	1D	Yes	1420542
Na	M, B	2	d [b]	Yes	2261695
Na	B, $\mu^{1,1}$, $\mu^{1,3}$	2	1D	Yes	1590315
Na	M, B	2	3D	Yes	1286014
Na	M, B	4	2D	Yes	1286015
Na	M, B	2	3D	Yes	1401350
Na	B	1	1D	Yes	266141
Na, Cs	B, $\mu^{1,1}$, $\mu^{1,3}$	5	3D	Yes	704680
K	B, $\mu^{1,1}$, $\mu^{1,3}$	2	3D	Yes	204441
K	B	1	3D	Yes	2050882
K, (Co) [d]	M, B	2	3D	Yes	678031
K	B, $\mu^{1,1}$, $\mu^{1,3}$	2	3D	Yes	967696
K	B, $\mu^{1,1}$, $\mu^{1,3}$	2	3D	Yes	1010829
K	B	1	d [b]	-	237164
K	M, B	2	2D	Yes	901373
K	M, B, $\mu^{1,3}$	4	3D	Yes	270823
K	B	1	d [b]	-	264947
K	B, $\mu^{1,1}$, $\mu^{1,3}$	6	3D	Yes	1165709
K	B, $\mu^{1,1}$, $\mu^{1,3}$	6	3D	Yes	214455
K	B, $\mu^{1,1}$, $\mu^{1,3}$	6	3D	Yes	1007783
K	M, B, $\mu^{1,1}$, $\mu^{1,3}$	3	3D	Yes	637403

K	B, $\mu^{1,1}$, $\mu^{1,3}$	1	3D	Yes	601424
K	M, B, $\mu^{1,1}$, $\mu^{1,3}$	7	3D	Yes	264106
K, (Zn) [d]	M, B, $\mu^{1,1}$, $\mu^{1,3}$	4	2D	No	2226952
K	B	2	d [b]	-	1420543
K, (U) [d]	M, B, $\mu^{1,1}$, $\mu^{1,3}$	3	3D	Yes	286236
K	B	1	3D	No	902017
K	B, $\mu^{1,1}$	3	2D	Yes	2261690
K	B, $\mu^{1,1}$, $\mu^{1,3}$	2	1D	Yes	1590316
K	B, $\mu^{1,1}$, $\mu^{1,3}$	2	1D	Yes	1590317
K	B	1	d [b]	-	1047335
K	B, $\mu^{1,1}$, $\mu^{1,3}$	4	3D	Yes	831174
K	M, B	2	3D	Yes	279861
K	B	1	2D	Yes	279863
K	B, $\mu^{1,1}$, $\mu^{1,3}$	1	3D	Yes	158300
K	B	3	3D	Yes	1022556
K	B, $\mu^{1,1}$, $\mu^{1,3}$	3	2D	Yes	781185
K	B	2	1D	Yes	290208
K	B	2	1D	Yes	605714
K	B	2	1D	Yes	974264
K	B, $\mu^{1,1}$, $\mu^{1,3}$	4	2D	Yes	1313529
K, Ba	B, $\mu^{1,1}$, $\mu^{1,3}$	1	3D	Yes	271589
K [c] (Mn) [d]	B, $\mu^{1,1}$, $\mu^{1,3}$	4	3D	Yes	2326580
K [c] (Ni) [d]	B, $\mu^{1,1}$, $\mu^{1,3}$	4	3D	Yes	2326581
Rb	M, B	3	1D	Yes	841082
Rb	B	1	3D	Yes	850376
Rb	B, $\mu^{1,1}$, $\mu^{1,3}$	3	3D	Yes	998206
Rb	B, $\mu^{1,1}$, $\mu^{1,3}$	3	3D	Yes	1010828
Rb	B	1	3D	Yes	834255
Rb	B	1	3D	Yes	1478712
Rb	B	1	d [b]	-	237165
Rb	B, $\mu_3^{1,1,1}$, $\mu^{1,3}$	2	2D	Yes	1153701
Rb	B, $\mu^{1,1}$, $\mu^{1,3}$	2	3D	Yes	1153745
Rb	M, B, $\mu^{1,1}$, $\mu^{1,3}$	3	3D	Yes	1153762
Rb	M, B, $\mu^{1,1}$, $\mu^{1,3}$	5	1D	Yes	1153775
Rb	M	1	1D	Yes	1169943

Rb (V)[d]	B, $\mu^{1,1}$, $\mu^{1,3}$	1	3D	Yes	222520
Rb	B, $\mu^{1,1}$, $\mu^{1,3}$	7	3D	Yes	264107
Rb	B, $\mu^{1,1}$, $\mu^{1,3}$	2	3D	Yes	674252
Rb	B, $\mu^{1,1}$, $\mu^{1,3}$	4	3D	Yes	290623
Rb	B, $\mu_3^{1,1,1}$, $\mu^{1,3}$	6	3D	Yes	979640
Rb	B, $\mu_3^{1,1,1}$, $\mu^{1,3}$	6	3D	Yes	979638
Cs	M, B	2	1D	Yes	1144482
Cs	B	1	3D	Yes	1478716
Cs	M, B, $\mu^{1,1}$, $\mu^{1,3}$	4	2D	Yes	1153763
Cs	M,B	2	1D	Yes	1169944
Cs	M, B	2	1D	Yes	2168841
Cs	B, $\mu_3^{1,1,1}$, $\mu^{1,3}$	2	3D	Yes	271508
Cs	M, B, $\mu^{1,1}$, $\mu^{1,3}$	3	3D	Yes	261542
Cs	B, $\mu_3^{1,1,1}$, $\mu^{1,3}$	6	3D	Yes	1516437
Cs	M, B, $\mu^{1,1}$, $\mu^{1,3}$	8	3D	Yes	264108
Sr	B	1	1D	No	1153815
Sr	B	1	d [b]	-	1153834
Sr	M, B	4	3D	Yes	610046
Ba	B	1	2D	Yes	1465130
Ba	B, $\mu^{1,1}$, $\mu^{1,3}$	2	2D	Yes	1128228
Ba	M, B	4	d [b]	-	1153839
Ba	M, B	6	3D	Yes	610047
Zn (Te) [d]	M, B	2	d [b]	-	1194896
Zn (Te) [d]	M, B	2	d [b]	-	1194897
Ag	B	1	2D	Yes	1186901
Ag	B	2	2D	Yes	1186904
Ag	B	2	2D	Yes	1186905

M = monodentate, B = bidentate, μ = bridging ligand. [a] Number of nitro groups attached to the metal atom, regardless of the coordination mode; [b] discrete arrangement (0D); [c] this work; [d] Heterometallic structures where the element in round brackets does not interact with the nitro group.

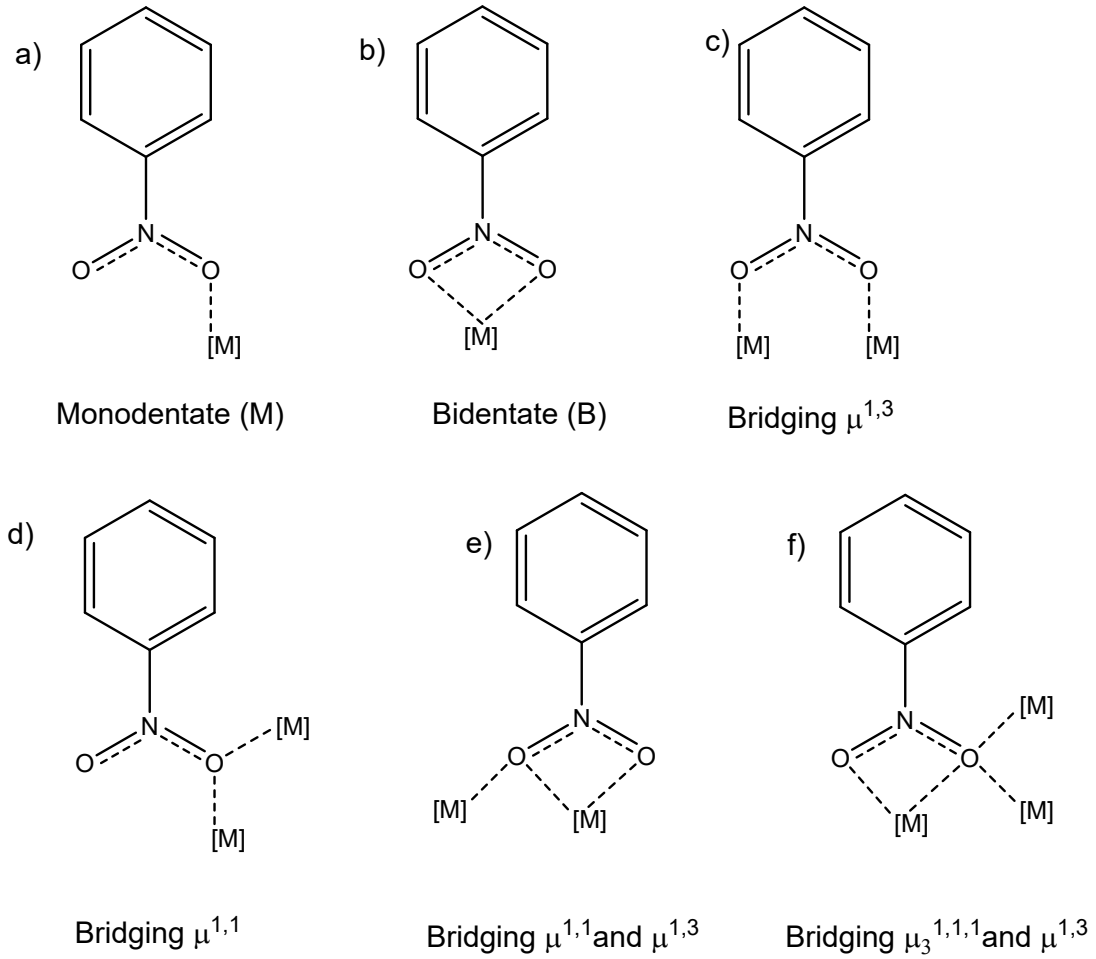

Figure S17. Main coordination modes of the nitro group (in nitrophenyl) present in the structures obtained from search in the CSD database (update June 2023).

6. IR spectroscopy characterization

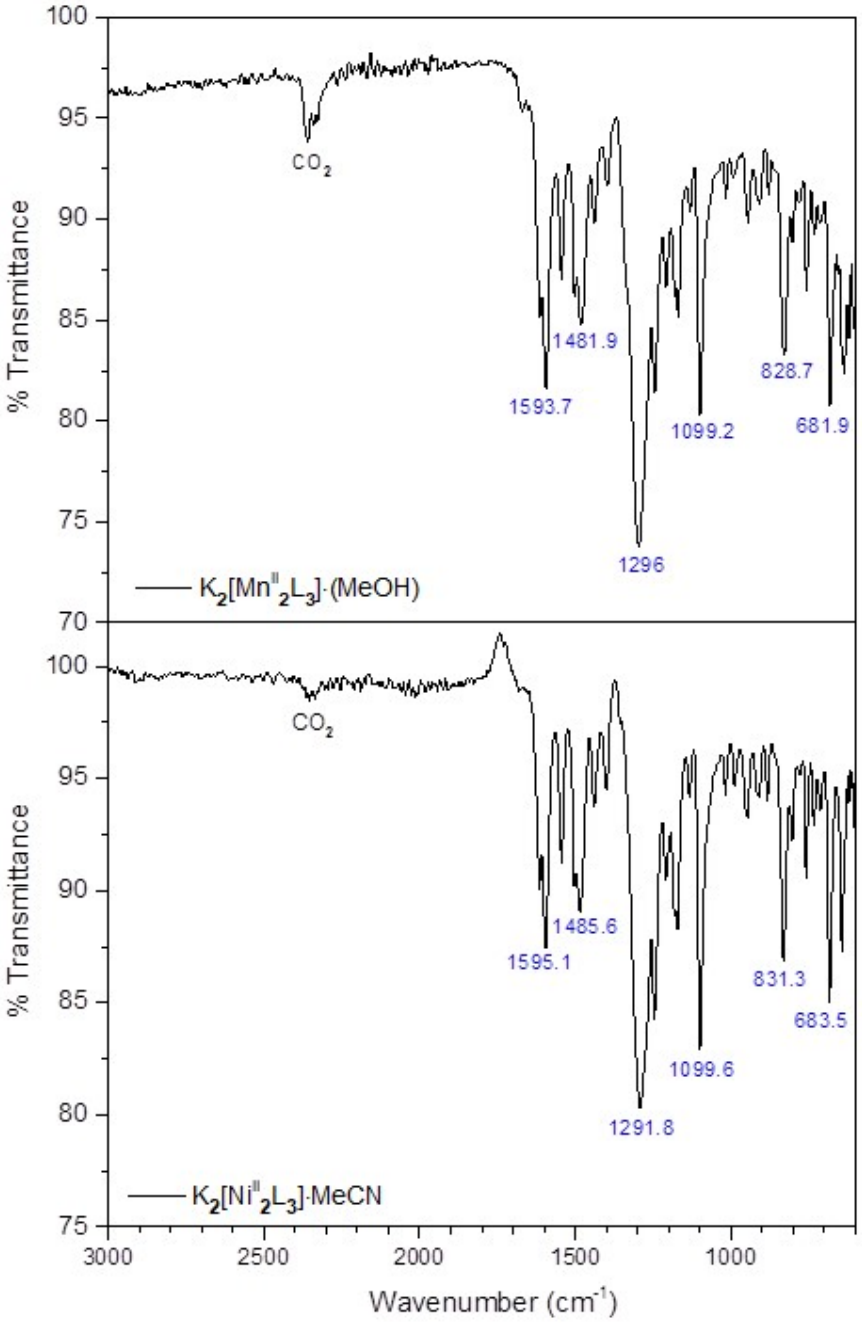

Figure S18. IR(ATR) spectra of complexes $K_2[Mn^{II}_2L_3]\cdot(MeOH)$ (**1**) (top) and $K_2[Ni^{II}_2L_3]\cdot(MeCN)$ (**2**) (bottom), showing inside the wavenumber values (cm^{-1}) of the most representative peaks.

7. References

S1. C. B. Hubschle, G. M. Sheldrick and B. Dittrich, *J. Appl. Crystallogr.*, 2011, **44**, 1281-1284.

S2. M. Mikuriya, K. Nakadera and T. Tokii, *Inorg. Chim. Acta*, 1992, **194**, 129-131.

S3. M. Mikuriya, T. Fujii, S. Kamisawa, Y. Kawasaki, T. Tokii and H. Oshio, *Chem. Lett.*, 1990, **19**, 1181-1184.

S4. B. Mabad, P. Cassoux, J. P. Tuchagues and D. N. Hendrickson, *Inorg. Chem.*, 1986, **25**, 1420-1431.

S5. P. Chakraborty, I. Majumder, K. S. Banu, B. Ghosh, H. Kara, E. Zangrando and D. Das, *Dalton Trans.*, 2016, **45**, 742-752.

S6. J. Adhikary, A. Chakraborty, S. Dasgupta, S. K. Chattopadhyay, R. Kruszynski, A. Trzesowska-Kruszynska, S. Stepanović, M. Gruden-Pavlović, M. Swart and D. Das, *Dalton Trans.*, 2016, **45**, 12409-12422.

S7. N. C. Jana, Z. Jagličić, P. Brandão, S. Adak, A. Saha and A. Panja, *New J. Chem.*, 2021, **45**, 7602-7613.

S8. M. Sebastian, V. Arun, P. P. Robinson, A. A. Varghese, R. Abraham, E. Suresh and K. K. M. Yusuff, *Polyhedron*, 2010, **29**, 3014-3020.

S9. P. Mukherjee, M. G. B. Drew, V. Tangoulis, M. Estrader, C. Diaz and A. Ghosh, *Inorg. Chem. Commun.*, 2009, **12**, 929-932.

S10. P. Ghorai, A. Chakraborty, A. Panja, T. K. Mondal and A. Saha, *RSC Advances*, 2016, **6**, 36020-36030.

S11. C. R. Martinez and B. L. Iverson, *Chem. Sci.*, 2012, **3**, 2191-2201.

S12. D. P. Malenov and S. D. Zarić, *Coord. Chem. Rev.*, 2020, **419**, 213338.